Developmental Cell, Volume *43*

Supplemental Information

Convergent Transcriptional Programs Regulate cAMP Levels in *C. elegans* GABAergic Motor Neurons

Bin Yu, Xiaolin Wang, Shuai Wei, Tao Fu, Emmanuel Enoch Dzakah, Ahmed Waqas, Walter W. Walthall, and Ge Shan

Supplemental Figure legends

Figure S1. CRISPR/cas9 knock-in of in-frame GFP & ChIP-seq peaks of known *unc-30* or *unc-55* targets (Related to Figure 1 and Figure 2)

(A) Diagram of GFP knock-in; F and R represent the detection primers. Gel analyses of UNC-30::GFP and UNC-55::GFP PCR productions are shown. The inserted *gfp* coding sequences are 717 bp.

(B) Western blots shown UNC-30::GFP and UNC-55::GFP fusion protein, along with actin as the loading control. UNC-30 itself should be ~35 KD, UNC-55 ~40 KD, and GFP ~26 KD; UNC-30::GFP fusion should be ~61 KD, and UNC-55::GFP fusion should be ~66 KD.

(C) Circos plots the distribution of UNC-30 and UNC-55 ChIP-seq signals around the genome.

(D) Venn diagram of UNC-30 and UNC-55 targeted coding, microRNA, and lincRNA genes.

(E) UNC-30 ChIP-seq peaks distribute on its targets.

(F) UNC-55 ChIP-seq peaks distribute on known *unc-55* targets. *hbl-1* and *unc-8* are suppressed by *unc-55* in VD MNs (Thompson-Peer et al., 2012; Miller-Fleming, et al., 2016). *unc-8*, *acr-2*, *slo-2*, *unc-129*, *dbl-1*, and *del-1* are regulated by *unc-55* in AS neurons (Kerk et al., 2017).

Figure S2. Transcriptional reporters of novel *unc-30* or *unc-55* targets (Related to Figure 2)

(A) Transcriptional reporters of some novel *unc-30* targets.

(B) Transcriptional reporters of some novel *unc-55* targets.

(C) Transcriptional reporters of *unc-30* and *unc-55* shared targets (*vhp-1*, *acr-14*, *myrf-1*, and *myrf-2*).

Figure S3. GO analyses of biological process of UNC-30 and UNC-55 target genes (Related to Figure 2)

(A) GO analysis of biological process of UNC-30 & UNC-55 shared targets (C1 in Figure 2).

(B) GO analysis of biological process of UNC-30 targets.

(C) GO analysis of biological process of UNC-55 targets.

(D) GO analysis of biological process of UNC-30 unique targets (C2 in Figure 2).

(E) GO analysis of biological process of UNC-55 unique targets (C3 in Figure 2).

Figure S4. Expression pattern of a longer *pde-4* promoter (*Ppde-4L*) and mutated *pde-4* promoter (*Ppde-4Δu55*), and *acy-1* as a common target of UNC-30 and UNC-55 (Related to Figure 3)

(A) *Ppde-4L::gfp* in *wild-type* and *unc-55(e1170)* adults. n=12 worms for each genotype. GFP intensity in arbitrary units (A.U.) normalized to *Punc-47*::RFP in D MNs of adult worms., n=*wild-type*, 12 worms, 12 DD, 16 VD; *unc-55(e1170)*, 12 worms, 10 DD, 17 VD. *Ppde-4L* is 6 kb, and the promoter (labeled as *Ppde-4*) used in Figure 3 and other experiments is 2.6 kb.

(B) Expression intensity of *Ppde-4Δu55*::GFP. n=23 *wild-type* worms, 50 VD.

(C) ChIP-seq peaks of UNC-30 and UNC-55 in *acy-1*.

(D) Plots of the *Pacy-1::gfp* expression levels along the time line are shown. n=26 DD (18 worms, 10h); 27 DD (20 worms, 14h); 26 DD (18 worms, 18h).

(E) Images of *Pacy-1::GFP* in *wild-type*, *unc-30(e191)*, and *unc-55(e1170)* adults. n=*wild-type*, 22 worms; *unc-55(e1170)*, 12 worms; *unc-30(e191)*, 10 worms. GFP intensities in arbitrary units (A.U.) normalized to *Punc-47*::RFP intensity in adults are shown in the plot figure. n=*wild-type*, 22 worms, 24 DD, 36 VD; *unc-55(e1170)*, 12 worms, 21 VD.

n.s., not significant; * $p<0.05$; *** $p<0.001$; One-Way ANOVA with Bonferroni correction. Scale bar, 20 μm.

Figure S5. Representative FRET images, FRET signals in D MNs of different genotypes, and presynaptic intensities of D MNs (Related to Figure 4); **VD aberrant remodeling in *pde-4(0)*, and FRET signals in D MNs of *oig-1* and *lin-14*** (Related to Figure 6)

(A) Representative FRET images along with the time line (hours after hatching) in *wild-type* DD MNs, the corresponding FRET signal is labeled below.

(B) FRET signals along the time line in DD or VD MNs in diverse backgrounds; time points are hours after hatch; n=37-42 DD MNs (33-37 worms), 36-45 VD MNs (30-34 worms) for *pde-4* mutants; 43-56 VD MNs (34-38 worms) for *wild-type*; 35-55

VD MNs (29-33 worms), for *unc-55* mutants.

(C) Images of *Punc-25::SNB-1::GFP* at different time points (post-hatch) in *wild-type* and *unc-55*. Statistics of GFP intensities are shown in the plot figure.

(D) Presynaptic SNB-1::GFP puncta in DNC in *wild-type* and *pde-4(0)*. Representative images are shown, and statistics of extra SNB-1::GFP puncta on dorsal side in *wild-type* and *pde-4(0)* are shown. L4 worms were examined; n=15 for each genotype. Asterisks indicate extra puncta (with P*unc-25*::SNB-1::GFP, without P*flp-13*::SNB-1::mCherry) from VD MNs with aberrant remodeling in *pde-4* mutant.

(E, F) FRET signals along the time line in DD or VD MNs in different backgrounds; time points are hours after hatch; n= 25-30 DD MNs (22-27 worms), 35-48 VD MNs (26-30 worms) for *oig-1* mutants; 25-30 DD MNs (25-29 worms) for *lin-14* mutants. Data in B are the same to Figure 6E for *oig-1* and *lin-14*, and data in C are the same to Figure 6F for *oig-1*.

Data are mean±S.E.M. for B-F; Student's t-test is used in D; One-Way ANOVA with Bonferroni correction is used in B, E, and F; Two-Way ANOVAwith Bonferroni correction for C. n.s. not significant, * $p<0.05$; ** $p<0.01$; *** $p<0.001$. Scale bar, 20 μm.

Figure S6. Deficiency of D MN respecification and cAMP levels in *pde-4;oig-1* double mutant (Related to Figure 7); ***lin-14* regulates *pde-4*, and *irx-1* regulates *acy-1*** (Related to Figure 7)

(A) Representative images of *wild-type* and *pde-4(0);oig-1(0).* Worms were 12 hour post-hatching.

(B) Representative images of *wild-type* and *pde-4(0);oig-1(0)* with presynaptic SNB-1::GFP puncta in VNC or DNC are shown. DNC, dorsal nerve cord; VNC, ventral nerve cord.

(C) FRET signals in 12h DD MNs and 28h VD MNs in different backgrounds; images taken from 12 hours; For DD MNs, n=24 (23 worms, *wild-type*), 36 (25 worms, *pde-4(0)*), 26 (24 worms, *oig-1(0)*), 27 (24 worms, *pde-4(0);oig-1(0)*). Images taken from 28 hours. For VD MNs, n= 42 (35 worms, *wild-type*), 36 (32 worms, *pde-4(0)*), 34 (27 worms, *oig-1(0)*), 28 (22 worms, *pde-4(0);oig-1(0)*). Data for *wild-type*, *pde-4*, and *oig-1* are the same as in Figures 6E, 6F, S5B, S5E and S5F.

(D) *Ppde-4::GFP* in *wild-type* and *lin-14(0)* L1 worms. n=15 worms, 22 DD for each

genotype.

(E) Images of *Pacy-1::GFP* in *wild-type* and *irx-1 csRNAi*. n=28 DD (20 worms *wild-type*), 31 DD (25 worms, *irx-1 csRNAi*)

Data are mean ± S.E.M. One-Way ANOVA with Bonferroni correction for C; Student's t-test for D and E. n.s., not significant; ** $p<0.01$; *** $p<0.001$. Scale bar, 20 μm.

Figure S7. Effects of ectopic *unc-55* expression, and comparison of UNC-30 & UNC-55 ChIP-seq targets to some related data (Related to Figure 7 and DISSCUSION)

(A) Expression of *Ppde-4*::GFP in control (*wild-type*, *Punc-47::RFP)* and UNC-55 ectopically expressed (*wild-type*, *Punc-47::UNC-55a::sl2::RFP*) worms. n=15 DD (12 worms, control) and 20 DD (15 worms, *Punc-47::unc-55a::sl2::RFP*).

(B) Statistics of *Pacy-1::GFP* fluorescence intensity in the control and UNC-55 ectopically expressed worms. n=28 DD (20 worms, *wild-type*) and 31 DD (26 worms, *Punc-47::unc-55a::sl2::RFP*).

(C) Representative images (time point of imaging at 24 hours) of T1 (ethanol control) and T2 (auxin treated) worms. Statistics of fluorescent intensity are shown, n=20 DD (15 worms, T1) and 22 DD (15 worms, T2). This panel is supplementary to Figure 7D. DNC, dorsal nerve cord. Dashed boxes are enlarged (DNC) to show presynaptic puncta. Solid boxes are enlarged to show DD2 and DD3 cell body, and the nuclear levels of UNC-55a::degron::GFP protein (labeled as UNC-55) are significantly decreased upon auxin induction.

(D) Venn diagram of 188 genes with elevated expression levels in VD MNs in *unc-55* mutant (Petersen et al., 2011) for their closest UNC-55 ChIP-seq binding peak. Eight genes (*T23B12.5*, *C10C5.2*, *F35D2.3*, *nspb-12*, *F53H4.3*, *kin-15*, *C50F7.5*, *D1079.1*) have UNC-55 binding peaks within 2.0 kb of their TSS.

(E) Venn diagram of UNC-30 ChIP targets, UNC-55 ChIP targets, and GABAergic neuron enriched genes in Cinar et al., 2005.

n.s., not significant; ** $p<0.01$; *** $p<0.001$; Student's t-test; data are mean ± S.E.M in A and B. data are mean ± SD in C. Scale bar, 20 μm.

Table S1 ChIP-seq peaks (related to Figure 1 and Figure 2).

Table S2 *C. elegans* strains (related to Star Methods).

Table S3 primer information (related to Star Methods).

Figure S1

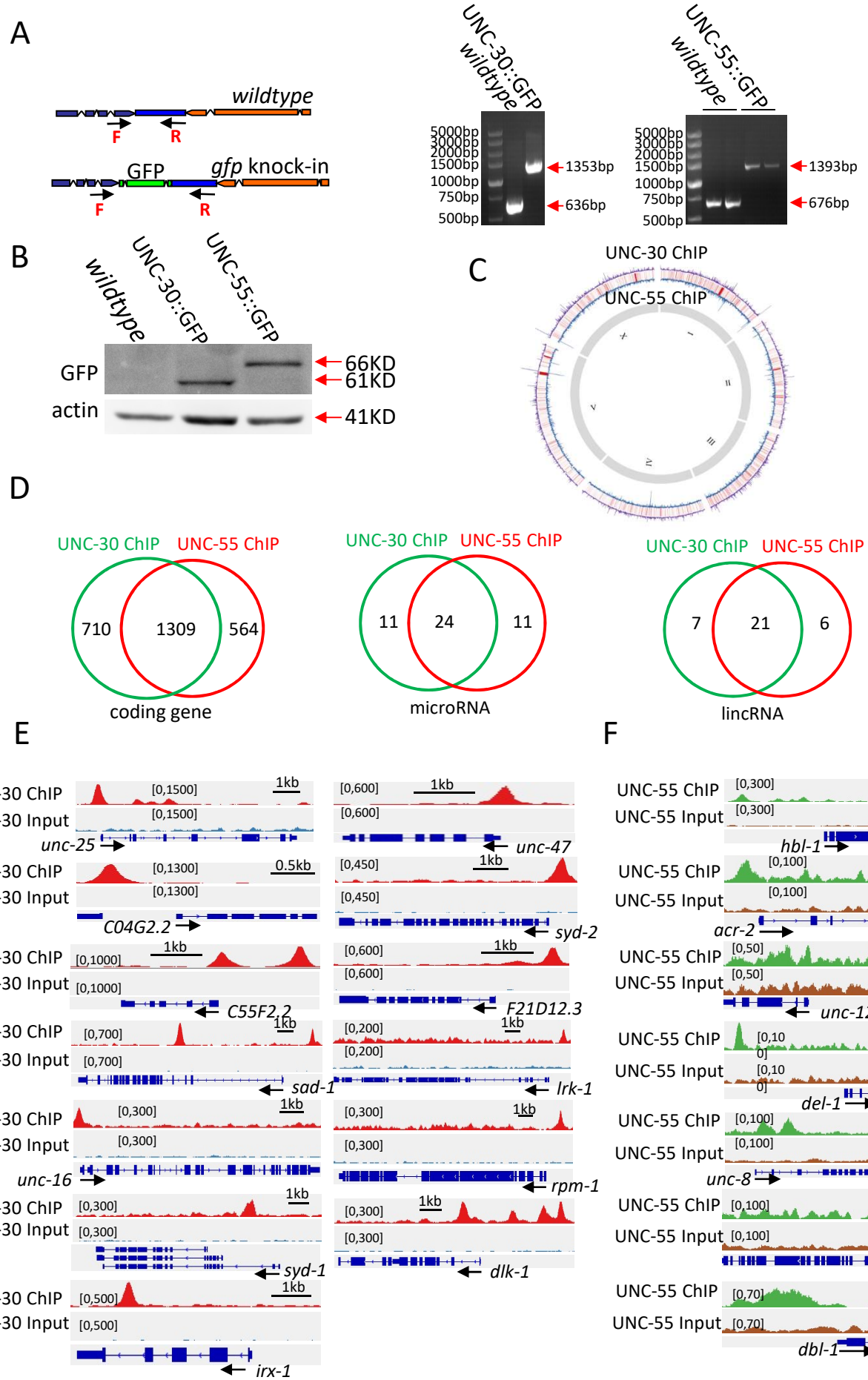
A
wildtype
F
R
GFP
gfp knock-in
F
R
UNC-30::GFP
wildtype
5000bp
3000bp
2000bp
1500bp
1000bp
750bp
500bp
1353bp
636bp
UNC-55::GFP
wildtype
5000bp
3000bp
2000bp
1500bp
1000bp
750bp
500bp
1393bp
676bp
B
wildtype
UNC-30::GFP
UNC-55::GFP
GFP
66KD
61KD
actin
41KD
C
UNC-30 ChIP
UNC-55 ChIP
D
UNC-30 ChIP
UNC-55 ChIP
710
1309
564
coding gene
UNC-30 ChIP
UNC-55 ChIP
11
24
11
microRNA
UNC-30 ChIP
UNC-55 ChIP
7
21
6
lincRNA
E
UNC-30 ChIP
UNC-30 Input
unc-25
[0,1500]
1kb
C04G2.2
[0,1300]
0.5kb
C55F2.2
[0,1000]
1kb
sad-1
[0,700]
1kb
unc-16
[0,300]
1kb
syd-1
[0,300]
1kb
irx-1
[0,500]
1kb
unc-47
[0,600]
1kb
syd-2
[0,450]
1kb
F21D12.3
[0,600]
1kb
lrk-1
[0,200]
1kb
rpm-1
[0,300]
1kb
dlk-1
[0,300]
1kb
F
UNC-55 ChIP
UNC-55 Input
hbl-1
[0,300]
1kb
acr-2
[0,100]
1kb
unc-129
[0,50]
1kb
del-1
[0,10
0]
1kb
unc-8
[0,100]
1kb
slo-2
[0,100]
1kb
dbl-1
[0,70]
0.5kb

Figure S2


A
UNC-30 ChIP
UNC-30 Input
[0,250]
0.5kb
bra-1
[0,150]
1kb
rgs-4
dhc-1
[0,1000]
lin-10
wildtype
unc-30(0)
Pbra-1::GFP
Punc-47::RFP
Prgs-4::GFP
Pdhc-1::GFP
Plin-10::GFP
B
UNC-55 ChIP
UNC-55 Input
[0,200]
lin-59
lin-18
[0,300]
vps-25
myrf-2
unc-55(0)
Plin-59::GFP
Plin-18::GFP
Pvps-25::GFP
Pmyrf-2::GFP
C
5kb
[0,600]
[0,220]
vhp-1
500bp
[0,800]
acr-14
myrf-1
Pvhp-1::GFP
Pacr-14::GFP
Pmyrf-1::GFP
VD9
VD10
VD11
DD5

Figure S3

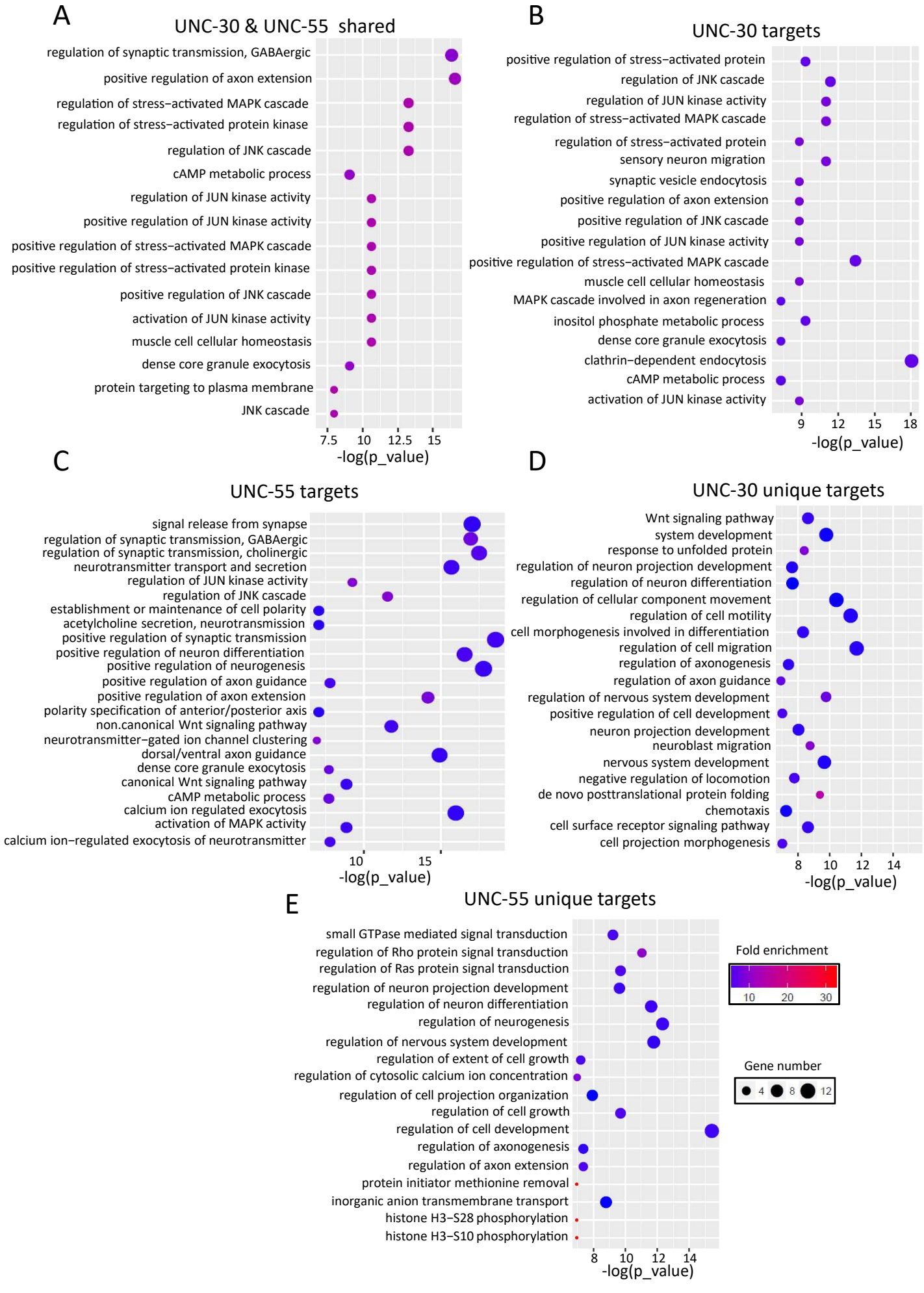
A
UNC-30 & UNC-55 shared
regulation of synaptic transmission, GABAergic
positive regulation of axon extension
regulation of stress−activated MAPK cascade
regulation of stress−activated protein kinase
regulation of JNK cascade
cAMP metabolic process
regulation of JUN kinase activity
positive regulation of JUN kinase activity
positive regulation of stress−activated MAPK cascade
positive regulation of stress−activated protein kinase
positive regulation of JNK cascade
activation of JUN kinase activity
muscle cell cellular homeostasis
dense core granule exocytosis
protein targeting to plasma membrane
JNK cascade
7.5
10
12.5
15
-log(p_value)
B
UNC-30 targets
positive regulation of stress−activated protein
regulation of JNK cascade
regulation of JUN kinase activity
regulation of stress−activated MAPK cascade
regulation of stress−activated protein
sensory neuron migration
synaptic vesicle endocytosis
positive regulation of axon extension
positive regulation of JNK cascade
positive regulation of JUN kinase activity
positive regulation of stress−activated MAPK cascade
muscle cell cellular homeostasis
MAPK cascade involved in axon regeneration
inositol phosphate metabolic process
dense core granule exocytosis
clathrin−dependent endocytosis
cAMP metabolic process
activation of JUN kinase activity
9
12
15
18
-log(p_value)
C
UNC-55 targets
signal release from synapse
regulation of synaptic transmission, GABAergic
regulation of synaptic transmission, cholinergic
neurotransmitter transport and secretion
regulation of JUN kinase activity
regulation of JNK cascade
establishment or maintenance of cell polarity
acetylcholine secretion, neurotransmission
positive regulation of synaptic transmission
positive regulation of neuron differentiation
positive regulation of neurogenesis
positive regulation of axon guidance
positive regulation of axon extension
polarity specification of anterior/posterior axis
non.canonical Wnt signaling pathway
neurotransmitter−gated ion channel clustering
dorsal/ventral axon guidance
dense core granule exocytosis
canonical Wnt signaling pathway
cAMP metabolic process
calcium ion regulated exocytosis
activation of MAPK activity
calcium ion−regulated exocytosis of neurotransmitter
10
15
-log(p_value)
D
UNC-30 unique targets
Wnt signaling pathway
system development
response to unfolded protein
regulation of neuron projection development
regulation of neuron differentiation
regulation of cellular component movement
regulation of cell motility
cell morphogenesis involved in differentiation
regulation of cell migration
regulation of axonogenesis
regulation of axon guidance
regulation of nervous system development
positive regulation of cell development
neuron projection development
neuroblast migration
nervous system development
negative regulation of locomotion
de novo posttranslational protein folding
chemotaxis
cell surface receptor signaling pathway
cell projection morphogenesis
8
10
12
14
-log(p_value)
E
UNC-55 unique targets
small GTPase mediated signal transduction
regulation of Rho protein signal transduction
regulation of Ras protein signal transduction
regulation of neuron projection development
regulation of neuron differentiation
regulation of neurogenesis
regulation of nervous system development
regulation of extent of cell growth
regulation of cytosolic calcium ion concentration
regulation of cell projection organization
regulation of cell growth
regulation of cell development
regulation of axonogenesis
regulation of axon extension
protein initiator methionine removal
inorganic anion transmembrane transport
histone H3−S28 phosphorylation
histone H3−S10 phosphorylation
8
10
12
14
-log(p_value)
Fold enrichment
10
20
30
Gene number
4
8
12

Figure S4

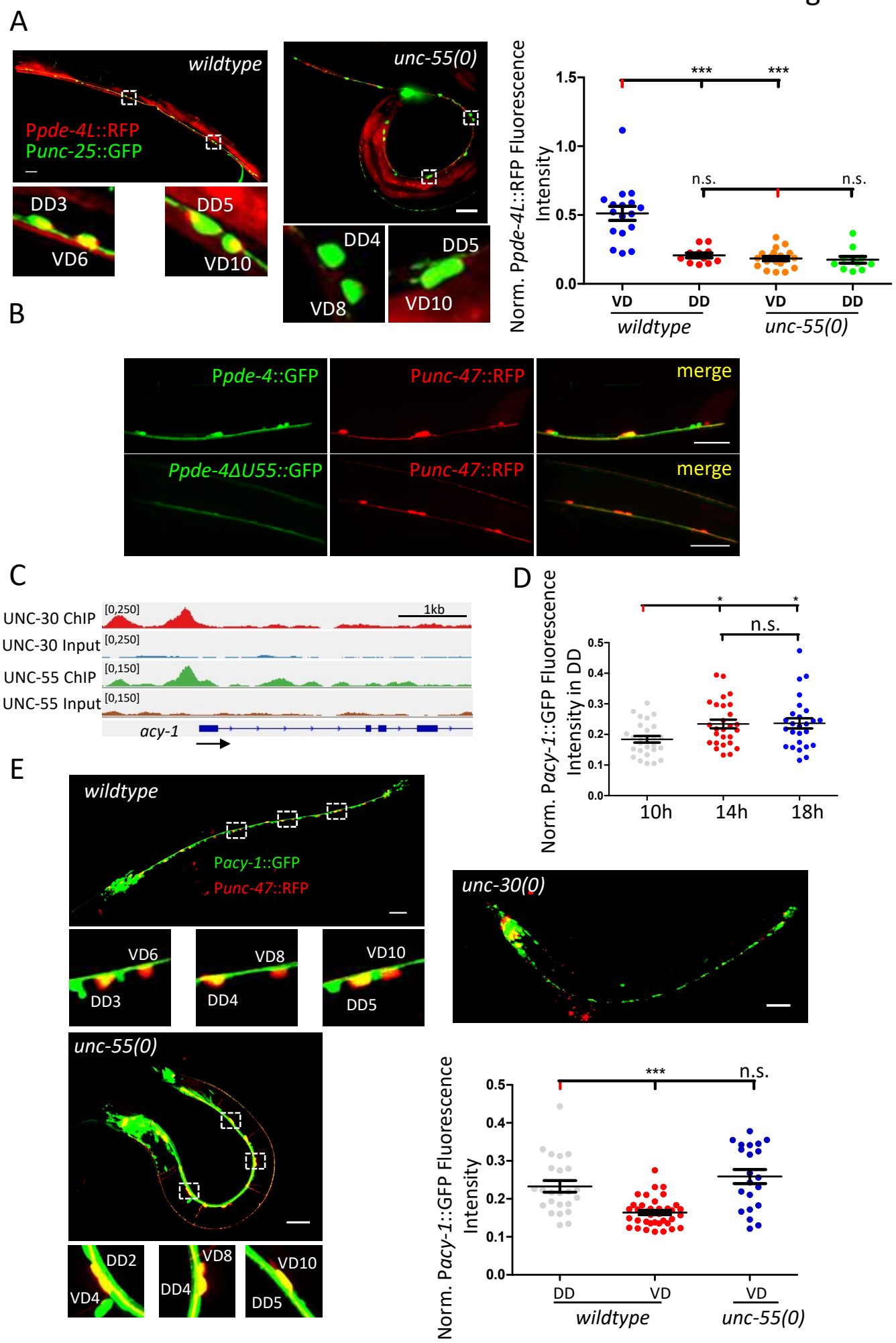
A
wildtype
Ppde-4L::RFP
Punc-25::GFP
DD3
VD6
DD5
VD10
unc-55(0)
DD4
VD8
DD5
VD10
Norm. Ppde-4L::RFP Fluorescence Intensity
1.5
1.0
0.5
0.0
***
***
n.s.
n.s.
VD
DD
VD
DD
wildtype
unc-55(0)
B
Ppde-4::GFP
Punc-47::RFP
merge
Ppde-4ΔU55::GFP
Punc-47::RFP
merge
C
UNC-30 ChIP
UNC-30 Input
UNC-55 ChIP
UNC-55 Input
[0,250]
[0,250]
[0,150]
[0,150]
1kb
acy-1
D
Norm. Pacy-1::GFP Fluorescence Intensity in DD
0.5
0.4
0.3
0.2
0.1
0.0
*
*
n.s.
10h
14h
18h
E
wildtype
Pacy-1::GFP
Punc-47::RFP
VD6
DD3
VD8
DD4
VD10
DD5
unc-30(0)
unc-55(0)
DD2
VD4
VD8
DD4
VD10
DD5
Norm. Pacy-1::GFP Fluorescence Intensity
0.5
0.4
0.3
0.2
0.1
0.0
***
n.s.
DD
VD
VD
wildtype
unc-55(0)

Figure S5

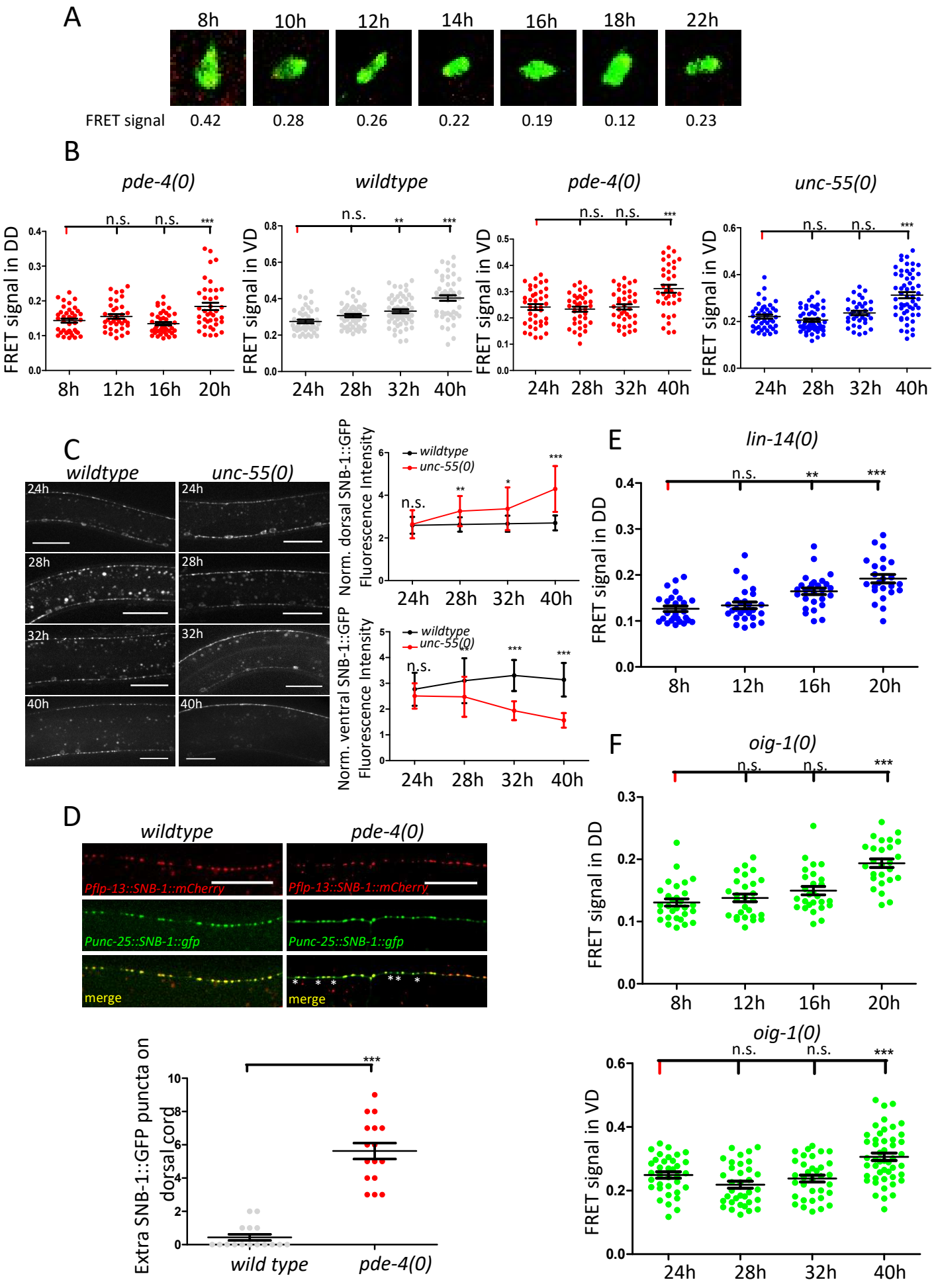
A
8h
10h
12h
14h
16h
18h
22h
FRET signal
0.42
0.28
0.26
0.22
0.19
0.12
0.23
B
pde-4(0)
wildtype
pde-4(0)
unc-55(0)
FRET signal in DD
FRET signal in VD
n.s.
**
***
8h
12h
16h
20h
24h
28h
32h
40h
C
wildtype
unc-55(0)
24h
28h
32h
40h
Norm. dorsal SNB-1::GFP Fluorescence Intensity
Norm. ventral SNB-1::GFP Fluorescence Intensity
wildtype
unc-55(0)
D
wildtype
pde-4(0)
Pflp-13::SNB-1::mCherry
Punc-25::SNB-1::gfp
merge
Extra SNB-1::GFP puncta on dorsal cord
wild type
pde-4(0)
E
lin-14(0)
F
oig-1(0)

Figure S6

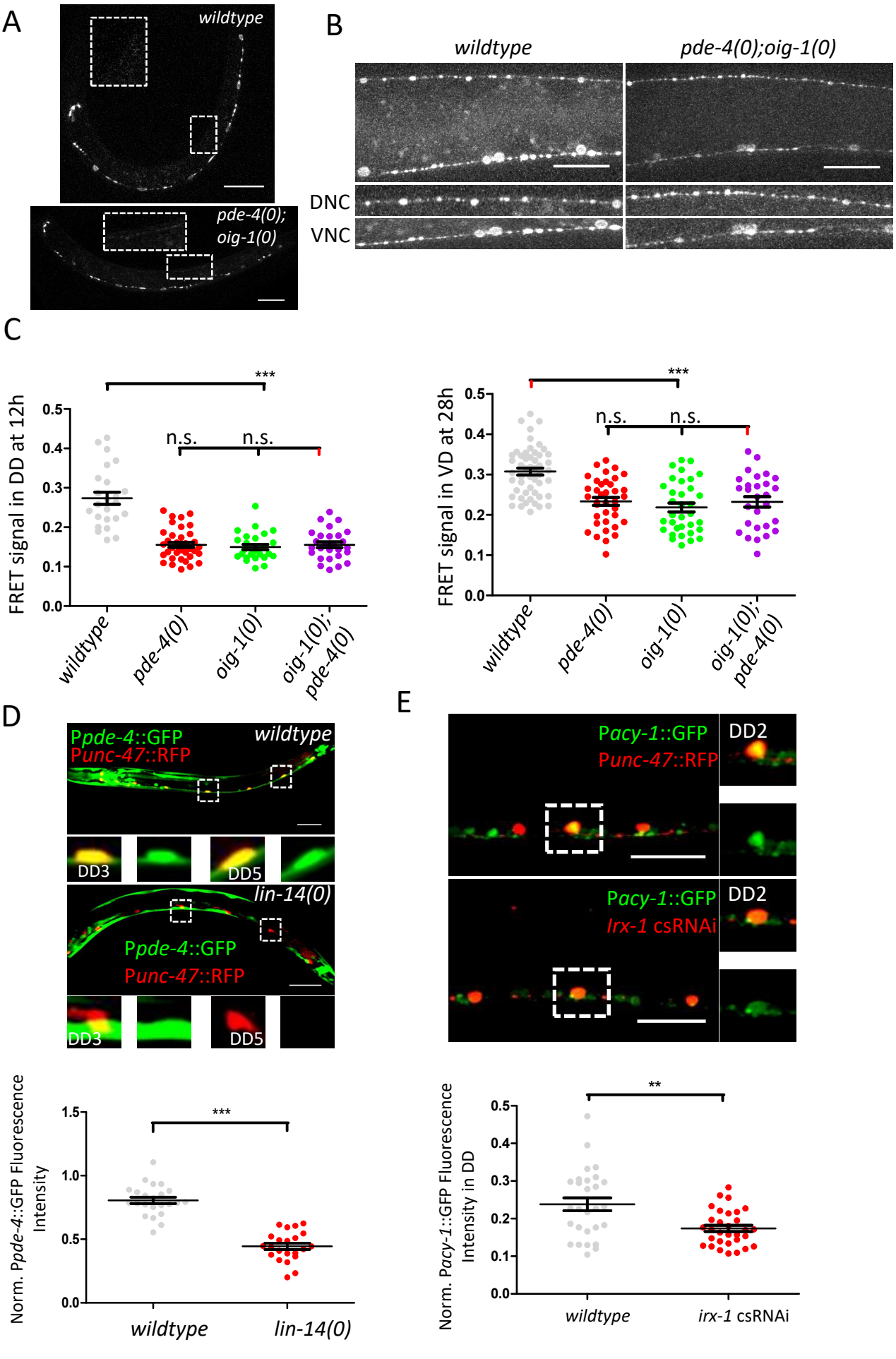
A
wildtype
pde-4(0);
oig-1(0)
B
wildtype
pde-4(0);oig-1(0)
DNC
VNC
C
FRET signal in DD at 12h
***
n.s.
n.s.
wildtype
pde-4(0)
oig-1(0)
oig-1(0);
pde-4(0)
FRET signal in VD at 28h
***
n.s.
n.s.
wildtype
pde-4(0)
oig-1(0)
oig-1(0);
pde-4(0)
D
Ppde-4::GFP
Punc-47::RFP
wildtype
DD3
DD5
lin-14(0)
Ppde-4::GFP
Punc-47::RFP
DD3
DD5
Norm. Ppde-4::GFP Fluorescence Intensity
***
wildtype
lin-14(0)
E
Pacy-1::GFP
Punc-47::RFP
DD2
Pacy-1::GFP
Irx-1 csRNAi
DD2
Norm. Pacy-1::GFP Fluorescence Intensity in DD
**
wildtype
irx-1 csRNAi

Figure S7

A

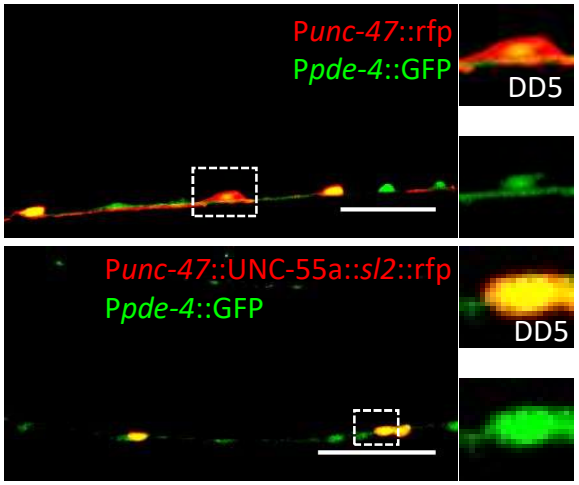

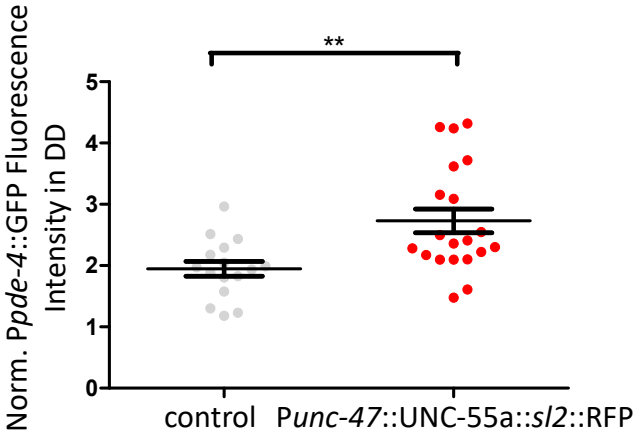

B

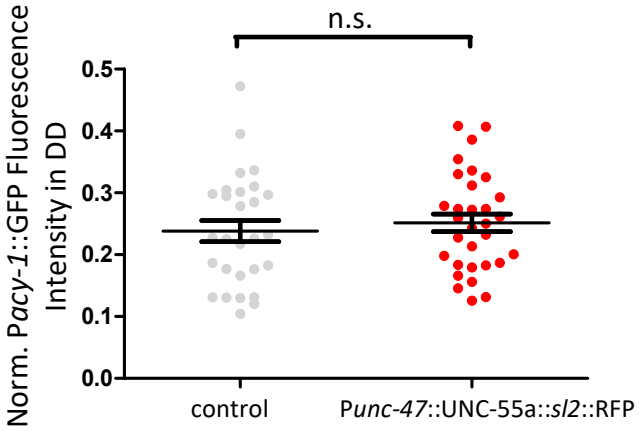

C

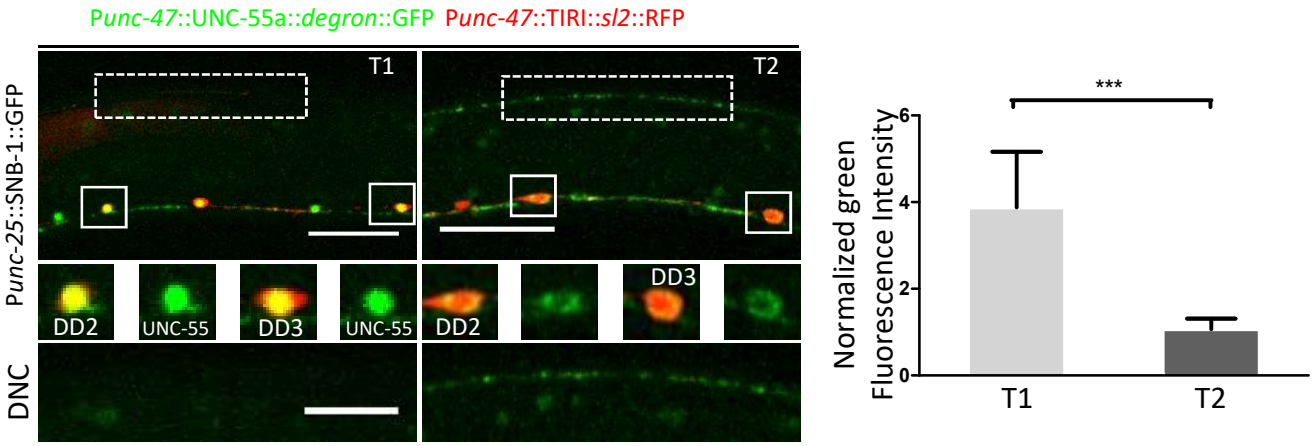

D

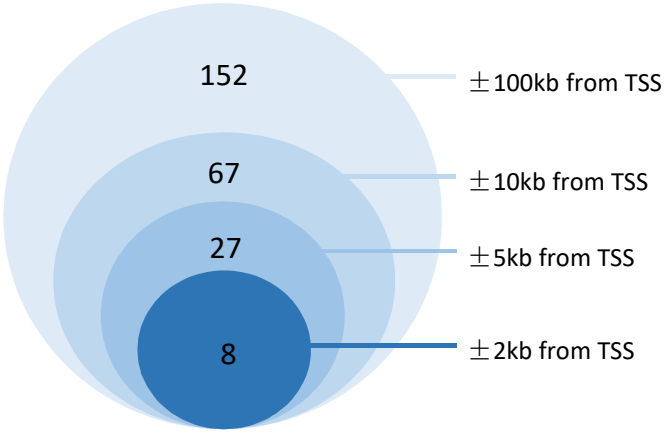

E